

## Electronic Supplementary Information

### **Porphyrin-based conjugated organic polymer with dual metal sites for visible-light-driven reduction of CO<sub>2</sub> to CO with highly active and selective**

Jinyu Li, Yuxia Hou,\* Cheng-Xing Cui, Xiupeng Zhang, Ji-Chao Wang, Airong Wang, Zhipeng Chen, Mingchang Li, and Tianjun Lou

---

J. Li, Y. Hou, C. Cui, X. Zhang, J. Wang, A. Wang, Z. Chen, M. Li, T. Lou

Department of Chemistry and Chemical Engineering

Henan Institute of Science and Technology

Xinxiang, 453003 (China)

\*Corresponding authors:

E-mail:

yxhou@hist.edu.cn

## **Physical measurements**

Fourier transform infrared (FT-IR) spectra were performed as KBr pellets using a Bruker Tensor 37 spectrometer with  $2\text{ cm}^{-1}$  resolution ( $m_{\text{Sample}}:m_{\text{KBr}}=1:100$ ). Powder X-ray diffraction (PXRD) data were collected on a Bruker D8 Advance XRD diffractometer using Cu-K $\alpha$  radiation ( $\lambda = 1.54060\text{ \AA}$ ) at room temperature. Transmission electron microscopy (TEM) images were measured on a JEOL JEM-2100 electron microscope operated at 200 kV. Scanning electron microscopy (SEM) images were obtained using a JEOL JEM-6510A scanning electron microscopy. For TEM imaging, a drop of freshly prepared sample solution was cast onto a carbon copper grid. For SEM imaging, a drop of freshly prepared sample solution was cast onto a silicon slice, and then Au (1-2 nm) was sputtered onto the grids to prevent charging effects and to improve the image clarity. X-ray photoelectron spectroscopy (XPS) was carried out on PHI 5300 ESCA System (Perkin-Elmer, USA). The excitation source is Al K $\alpha$  radiation. Metal content was determined by Optima 2100DV inductively coupled plasma atomic emission spectrometry (ICP), by digesting the sample in concentrated nitric acid.

## **Photoelectrochemical characterization.**

The photocurrent measurement were performed on three-electrode system using an electrochemical workstation. The cleaned ITO glass deposited with samples, Pt and Ag/AgCl electrode were used as working electrode, counter electrode, and reference electrode, respectively. The light source was a 300 W Xe lamp equipped with an ultraviolet cutoff filter ( $> 400\text{ nm}$ ) and 0.5 M Na<sub>2</sub>SO<sub>4</sub> aqueous solution acted

as the electrolyte.

Entry	Catalysts	SA	Main Product	Wavelength (nm)	Activity ( $\mu\text{mol g}^{-1} \text{h}^{-1}$ )	Selectivity (%)	Ref
1	Co-POM	TEOA	CO	400 ~ 800	17	80	1
2	TTCOF- Zn	H <sub>2</sub> O	CO	420 ~ 800	2.06	100	2
3	Azo-Por- Bpy-POP	H <sub>2</sub> O	CO	> 400 nm	38.75	100	3
4	CdS- EF/FeTCP P	TEOA	CO	420 ~ 780	7.5	88	4
5	ZrPP-1- Co	TEOA	CO	> 420	14	96.4	5
6	CuTBPP- DTBP-Co	H <sub>2</sub> O	CO	> 400 nm	32.5	100	<b>This Work</b>

**Table. S1** Photocatalytic activity and selectivity of CO<sub>2</sub> reduction in reported heterogeneous systems.

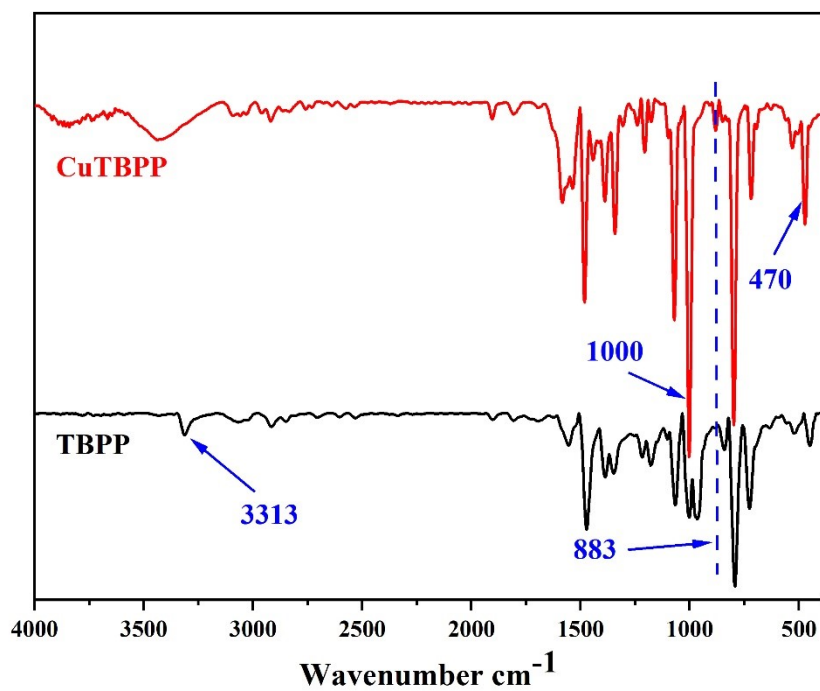


**Fig. S1** IR spectra of CuTBPP and TBPP. The IR spectrum of TBPP showed that the characteristic N-H stretching vibration at 3313  $\text{cm}^{-1}$  of TBPP disappeared after the reaction, N-Cu and C-Br stretching vibration of CuTBPP at 883  $\text{cm}^{-1}$  and 470  $\text{cm}^{-1}$ , 1000  $\text{cm}^{-1}$  for porphyrin skeleton vibration.

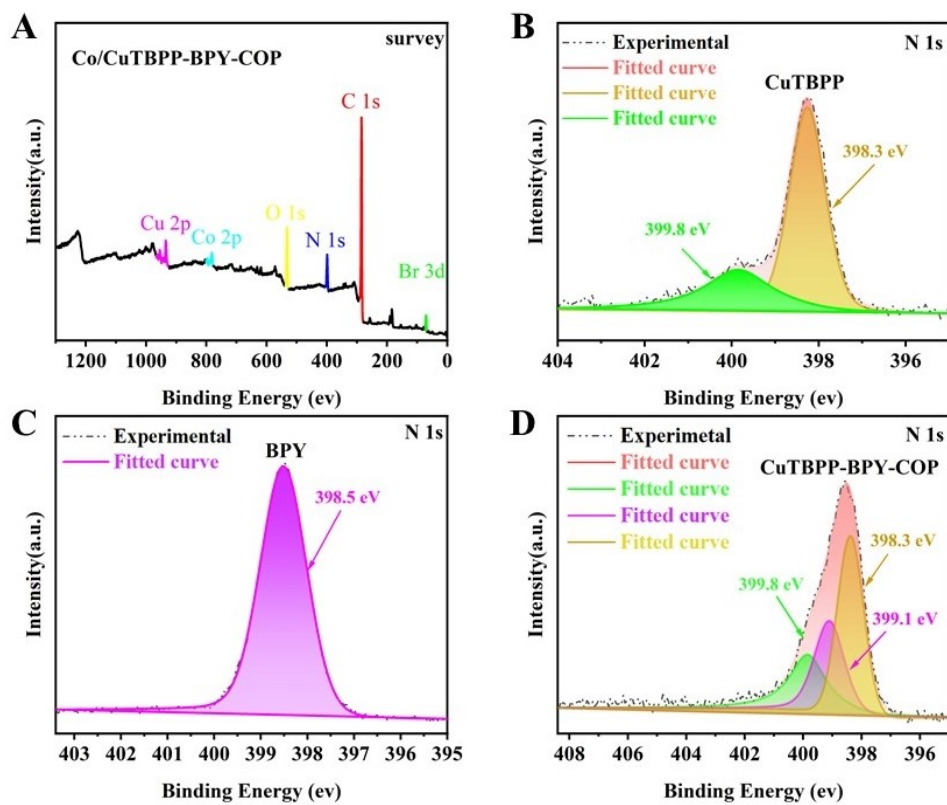


**Fig. S2** (A) XPS survey spectrum of Co/CuTBPP-BPY-COP (B) N 1s XPS spectrum of CuTBPP. (C) N 1s XPS spectrum of BPY. (D) N 1s XPS spectrum of CuTBPP-BPY-COP.

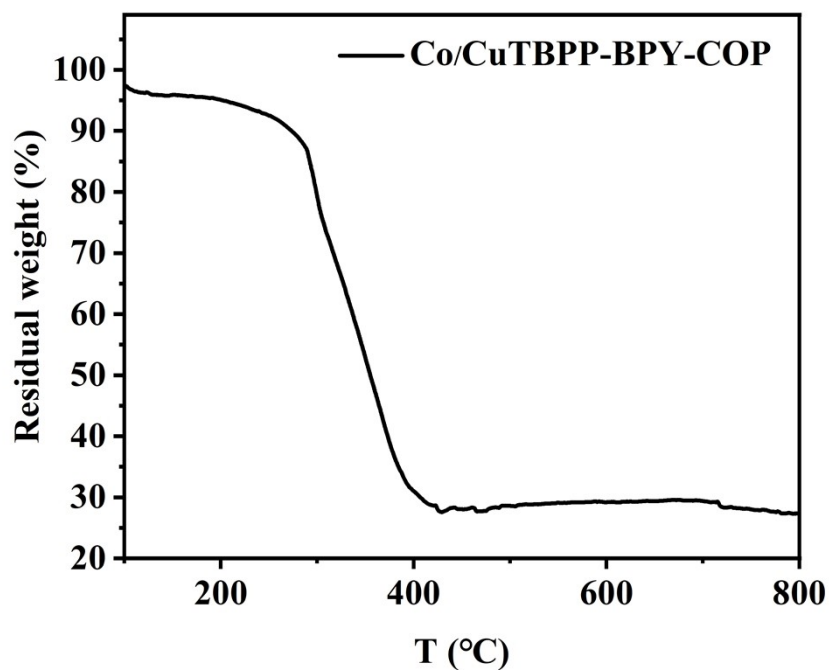


**Fig. S3** Thermogravimetric analysis (TGA) data of Co/CuTBPP-BPY-COP.

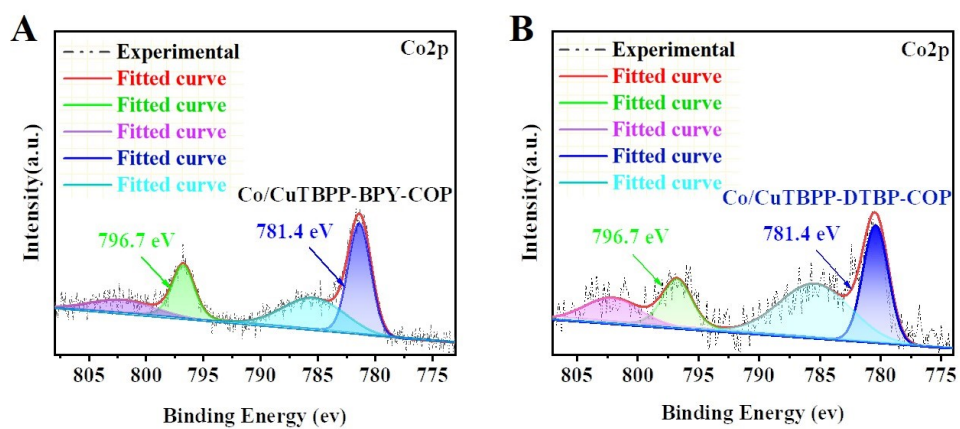


**Fig. S4** XPS spectra of the Co 2p region for Co/CuTBPP-BPY-COP after (B) and before (A) photocatalysis.

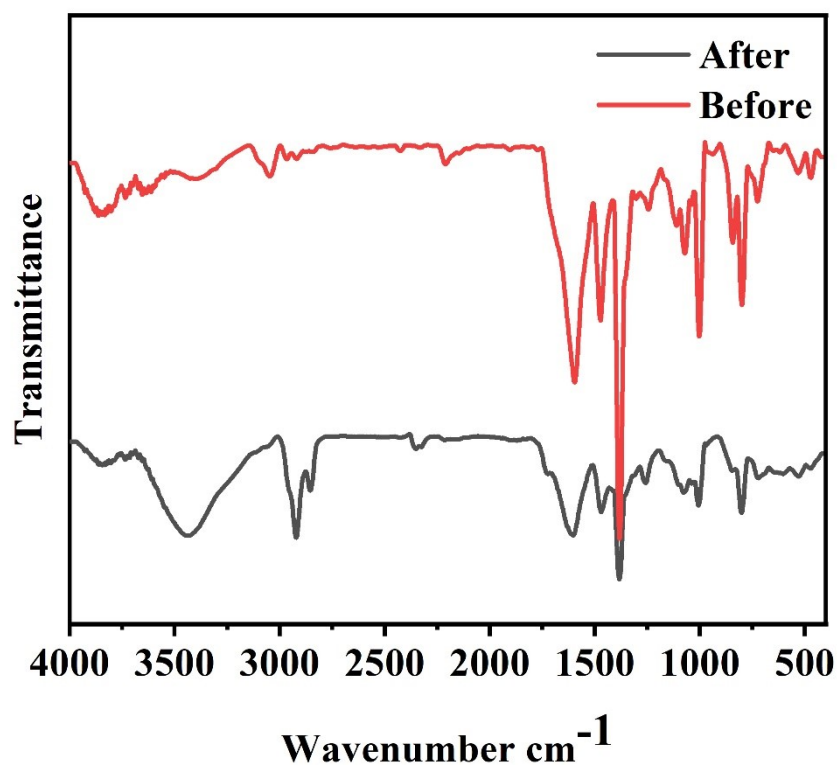


**Fig. S5** The FT-IR spectra of Co/CuTBPP-BPY-COP after (red) and before (black) photocatalysis.

Sample	Co amount by ICP (wt%)	CO <sub>2</sub> reduction efficiency (μmol g <sup>-1</sup> )
Co/CuTBPP-BPY-COP-1	0.26	64.6
Co/CuTBPP-BPY-COP-2	0.55	78.9
Co/CuTBPP-BPY-COP	0.77	130.1

**Table. S2** ICP analysis result of Co/CuTBPP-BPY-COP-1, Co/CuTBPP-BPY-COP-2 and Co/CuTBPP-BPY-COP.

1. G. Zhao, H. Pang, G. Liu, P. Li, H. Liu, H. Zhang, L. Shi and J. Ye, *Applied Catalysis B: Environmental*, 2017, **200**, 141-149.
2. M. Lu, J. Liu, Q. Li, M. Zhang, M. Liu, J. L. Wang, D. Q. Yuan and Y. Q. Lan, *Angewandte Chemie International Edition*, 2019, **58**, 12392-12397.
3. Y. Hou, E. Zhang, J. Gao, S. Zhang, P. Liu, J.-C. Wang, Y. Zhang, C.-X. Cui and J. Jiang, *Dalton Transactions*, 2020, **49**, 7592-7597.
4. P. Li, C. Hou, X. Zhang, Y. Chen and T. He, *Applied Surface Science*, 2018, **459**, 292-299.
5. E.-X. Chen, M. Qiu, Y.-F. Zhang, Y.-S. Zhu, L.-Y. Liu, Y.-Y. Sun, X. Bu, J. Zhang and Q. Lin, *Advanced Materials*, 2018, **30**, 1704388.